

New Hybrid Organic-inorganic Multifunctional Materials Based on Polydopamine-like Chemistry

Carla Calabrese,^[a] Leonarda Francesca Liotta,^[b] Loraine Soumoy,^[c] Carmela Aprile,^[c] Francesco Giacalone,^{*[a]} and Michelangelo Gruttadauria^{*[a]}

Abstract: A simple one-pot procedure under mild conditions has been developed with the aim of preparing a set of hybrid organic-inorganic multifunctional materials. This procedure is based on the use of catechol and KIO_4 as oxidizing agent in conjunction with 3-aminopropyl-, substituted 3-aminopropyl- and 3-methylimidazolium-1-trimethoxypropylsilane mimicking polydopamine-like chemistry. Reactions were carried out in water at room temperature and 70°C to give fifteen materials that were characterised by using several techniques

(nitrogen physisorption, TGA, XPS, ^{13}C and ^{29}Si CP-MAS NMR, IR, pH_{pzc}). Knoevenagel reaction was chosen as a good probe to investigate the availability of functional groups on the surface of the materials. The most active catalytic materials were tested in recycling procedures. Such simple procedure is of broad interest for the scientific community and it opens the doors to the development of new hybrid organic-inorganic multifunctional materials for several purposes.

Introduction

The continuous development of new materials for catalytic applications as well as other purposes is a topic of great interest and, in this context, great attention has been focused on the design of hybrid organic-inorganic materials for organocatalytic and metal-based reactions.^[1] Among the plethora of new materials, in the last decade, a paramount attention has been devoted to the so-called mussel-inspired materials based on polydopamine (PDA) or polydopamine-like polymers^[2] which also show high potential as catalysts in sustainable chemistry.^[3] The sustainability of catalytic processes is mainly based on the easy and, possibly, cheap and green synthesis of the catalytic materials then coupled with high catalytic activity, recoverability and reusability. In this context, oxidation of dopamine or simple catechol-based compounds to give polydopamine or polydopamine-like materials could be an appealing approach. In place of dopamine, the use of simple catechol, as an

alternative source of the catechol moiety, requires the presence of amine-based derivatives in the co-polymerisation processes leading to the formation of the desired polymeric material.^[4] The nature, quite complex, of these materials was also investigated using 4-methyl catechol and propylamine as model compounds.^[5] It is known that primary amines can covalently bind to polydopamine analogously to the ring formation in PDA itself.^[6] In addition to simple amines, 3-aminopropyltriethoxysilane, mainly as triethoxysilane (APTES), has been used in conjunction with dopamine, tannic acid or 5,6-dihydroxyindole-2-carboxylic acid for the development of new materials for selected applications.^[7]

Due to the great interest in mussel-inspired chemistry, we recently reported a simple and low-cost approach by using the cheap catechol and 3-aminopropyltrimethoxysilane (APTMS), as the amine counterpart, for the synthesis of a polydopamine-like silica-based material.^[8]

Then, we started a deeper investigation in the development of new hybrid organic-inorganic multifunctional materials in a very easy way. Indeed, oxidation-polymerisation of catechol followed by nucleophilic addition of amine moiety and hydrolytic polycondensation of trimethoxysilane group can give a final material displaying several functional groups such as amine, imine, phenolic hydroxyl as well as carbonyl groups. Indeed, multifunctional materials are very appealing for cooperative catalysis.^[1a,9] In order to test the new synthesised materials, Knoevenagel reaction was chosen as a good probe to investigate the availability of functional groups on the surface of the materials. Knoevenagel reaction may take place through several pathways and it is a very useful reaction for the total synthesis of biologically active natural products and their synthetic analogues, electroluminescent compounds, for organic solar cells and in medicinal chemistry among other applications.^[10]

[a] Dr. C. Calabrese, Prof. F. Giacalone, Prof. M. Gruttadauria
Department of Biological, Chemical and Pharmaceutical Sciences and Technologies
University of Palermo
Viale delle Scienze, Ed. 17, 90128, Palermo (Italy)
E-mail: francesco.giacalone@unipa.it
michelangelo.gruttadauria@unipa.it

[b] Dr. L. F. Liotta
Istituto per lo Studio dei Materiali Nanostrutturati
ISMN-CNR
Via Ugo La Malfa 153, 90146 Palermo (Italy)

[c] L. Soumoy, Prof. C. Aprile
Laboratory of Applied Materials Chemistry (CMA)
Department of Chemistry, University of Namur
61 rue de Bruxelles, 5000 Namur (Belgium)

Supporting information for this article is available on the WWW under <https://doi.org/10.1002/ajoc.202100443>

© 2021 The Authors. Asian Journal of Organic Chemistry published by Wiley-VCH GmbH. This is an open access article under the terms of the Creative Commons Attribution License, which permits use, distribution and reproduction in any medium, provided the original work is properly cited.

Results and Discussion

Hybrid materials were easily obtained with a one-pot procedure under mild conditions. In the first step, catechol was dissolved in $\text{KHCO}_3/\text{K}_2\text{CO}_3$ buffer solution (10 mM, pH 9.0) and, with the aim of forming enough *o*-quinone, the oxidant KIO_4 was added at room temperature. The solution turned very dark in a few minutes and it was left to stir for 2.5 h. In the second step, to this dark solution, the proper trimethoxysilane derivative was added and the solution was stirred at 70°C for 18 h. After this time, brown or dark-brown precipitates were formed which were easily filtered, washed and dried to give the hybrid materials. As trimethoxysilane derivative, the following aminopropyltrimethoxysilane **A–E** were used (Figure 1). In addition, imidazolium-based silanes **F–H** were also used.

Materials were prepared using only one silane (**A–E** entries 1–10) or a mixture of two silanes (entries 11–15). Materials were labelled with the letter of the silane employed with a different number (0, 1, 2) depending on the amount of oxidizing agent used and with additional letter *d* when the concentration was doubled (see Table 1). For the synthesis of the **A0** solid (Table 1, entry 1) no oxidizing agent was used, the oxidation/polymerisation reaction of the catechol took place by means of atmospheric oxygen in 100 mL of buffer solution at room temperature for a duration of 24 h, after which no

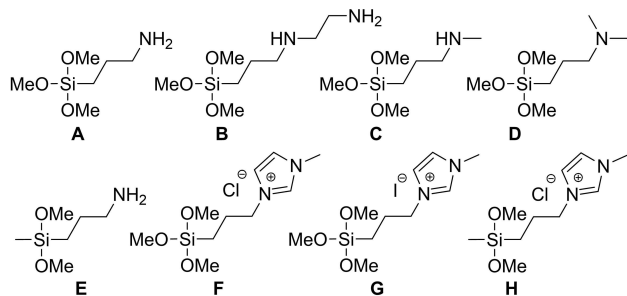


Figure 1. Structure of silanes **A–H**.

precipitate was observed. Subsequently, 3-aminopropyltrimethoxysilane (**A**) (10 mmol) was added as crosslinking agent and the reaction continued for 18 h at a temperature of 70°C .

The subsequent materials (**A1** and **A2**, entries 2 and 3) were prepared using silane **A**, in the presence of variable amount of KIO_4 (0.25 and 0.50 equivalent with respect to catechol). In these cases, the oxidation was very fast. The use of periodate as oxidant was reported also to accelerate the oxidation of dopamine.^[11] In our case, the mixture immediately became very dark and the reaction was carried out for 2.5 h at room temperature, after which, silane **A** was added and the reaction set at 70°C for 18 h. The reaction carried out with 0.50 equivalents of oxidant (entry 3) provided a greater amount of final material (**A2**). For this reason, subsequent tests were conducted using 0.50 equivalents (see Table 1).

For the synthesis of **B2** (entry 4) silane **B**, having two amino groups, secondary and primary, was used. Silane **C**, having a secondary amino group, was used for the preparation of **C2** (entry 5) whereas silane **D**, having a tertiary amino group, was used in the synthesis of **D2**. Given the lower amount of material obtained in the latter case (entry 6), the synthesis was repeated by halving the volume of the buffer solution used, 50 mL rather than 100 mL. However, solid **D2d** was obtained in a similar amount (entry 7). Finally, the synthesis of **E2** (entry 8) was carried out by adding the silane **E**, which possesses a dimethoxymethyl silane moiety instead of the trimethoxysilane.

The choice of using such silane was made in an attempt to obtain a polymer with a lower degree of branching; the absence of the third methoxy group bonded to silicon can result in the obtaining of a more linear polymeric structure, and in this way guaranteeing the material a greater contact surface and making the amino functionalities more accessible. In addition, the presence of the methyl group in place of the methoxy one could increase the hydrophobicity of the final material. The synthesis was repeated by doubling the concentration to give **E2d** (entry 9); the amount of material obtained using this procedure remained constant. On the other hand,

Entry	Silane	Material	KIO_4 /buffer [eq./mL]	Weight ^[b] [g]	Residue ^[c] [%]	Loading ^[d] [mmol/g]	Amt. H_2O ^[c] [%]
1	A	A0	0/100	0.820	49.2	8.2	5.7
2	A	A1	0.25/100	0.930	39.7	6.6	6.3
3	A	A2	0.50/100	1.390	36.6	6.1	7.0
4	B	B2	0.50/100	1.023	28.2	4.7	5.8
5	C	C2	0.50/100	0.917	32.4	5.4	7.0
6	D	D2	0.50/100	0.586	21.5	3.6	7.4
7	D	D2d	0.50/50	0.545	21.3	3.6	7.0
8	E	E2	0.50/100	1.200	36.9	6.1	3.3
9	E	E2d	0.50/50	1.203	39.7	6.6	2.6
10	E	E1d	0.25/50	0.743	40.4	6.7	2.5
11	A + D ^[e]	AD6.5	0.50/100	1.380	39.8	6.6	3.5
12	A + F ^[e]	AF6.5	0.50/100	1.230	33.1	5.2	4.0
13	A + F ^[f]	AF1.10	0.50/100	0.700	17.4	2.9	3.5
14	A + G ^[e]	AG6.5	0.50/100	1.300	33.7	5.6	4.1
15	E + H	EH6.5	0.50/100	0.950	30.9	5.1	2.8

[a] Reaction conditions: Catechol (4.36 mmol), buffer solution ($\text{KHCO}_3/\text{K}_2\text{CO}_3$, pH 9, 10 mM, 100 mL or 50 mL), KIO_4 (0.5 or 0.25 eq), r.t., 2.5 h; organosilane (10 mmol), 70°C , 18 h. [b] Isolated weight. [c] Calculated by TGA. [d] Silane loading from TGA, calculated from the residue at 800°C . [e] Silanes amount: 6 mmol + 5 mmol, respectively. [f] Silanes amount: 1 mmol + 10 mmol, respectively.

lower amount of material was obtained when less amount of oxidant was used (**E1d**, entry 10). This result resembles the one reported in entry 2.

Materials were also prepared using a mixture of two silanes. These solids are labelled with letters of the corresponding silanes and two numbers which correspond their molar ratio. In order to get a material having primary and tertiary amino groups, a mixture of silane **A** and silane **D** was used. The use of silane **A** together with silane **D** allowed to get a higher amount of material **AD6.5**. Solids **AF6.5**, **AF1.10** and **AG6.5** were prepared using silane **A** and imidazolium-based silanes **F** and **G** (entries 12–14). In the case of **AF1.10**, a large amount of silane **F** was used compared to silane **A** (**A:F** 1:10 mmol ratio). In this case, a lower amount of material was obtained (entry 13). Finally, material **EH6.5** was obtained from dimethoxymethylsilanes **E** and **H** (entry 15).

The hybrid materials were characterised by using several techniques confirming the presence of different functional groups. Firstly, materials were characterised by thermogravimetric analysis (TGA). Thermograms are reported in the Electronic Supporting Information (ESI) section (Figure S1), and the results are collected in Table 1. The first weight loss, observed around 100 °C, corresponds to the water adsorbed by the materials. The amount of adsorbed water could be a rough indication of hydrophilicity or hydrophobicity of the surfaces.^[12] The lower amount of adsorbed water the higher hydrophobicity. Dimethoxymethyl-based silica materials (**E2**, **E2d**, **E1d** and **EH6.5**), as expected, showed higher hydrophobicity (entries 8–10, 15). The residue values were corrected based on the amount of water present in the samples. The materials have a good thermal stability being stable up to 200 °C; the organic portion is completely degraded at 700 °C. In order to verify the reproducibility of the procedure, repeated preparation of the materials gave similar results.

The percentages of the obtained residue are reported in Table 1. This value is related to the residual silica (SiO₂) that corresponds to the alkoxy silane used in the synthesis. These data allowed to calculate the silane loading in the materials. As a first approximation, these values can also be correlated to the amount of amine present, although the possibility that Michael addition reactions occurred means that the amino functions present in the material are not all the same and not equally available on the surface of the materials.

The material obtained in the absence of the oxidizing agent (entry 1) has a very high residue, probably due to the fact that only a small amount of oxidised catechol was present in the

reaction system, i.e. quinone structures and/or oxidised polycatechol with which the APTMS could have reacted. The use of KIO₄ has provided materials with a lower silane loading, due to the presence of higher polycatechol/quinone structures with which the APTMS was able to react (entries 2 and 3). The use of silane **B**, containing two amino functions, primary and secondary, has provided a material with a lower loading (entry 4). The reaction was duplicated, obtaining a comparable result. The loading was slightly higher (entry 5) when silane **C** was used, having only a secondary amino function. The use of silane **D**, having a tertiary amine, has provided a material with a low silane loading (entry 6). This result was predictable since the primary and secondary amino functions can give nucleophilic addition reactions (Michael addition) on the α , β -unsaturated carbonyl systems of the quinone systems. Furthermore, primary amines can form imines with the ketone groups of such systems. Tertiary amines cannot give addition reactions to the carbonyl and certainly Michael's addition is less likely. This explains the smaller amount of the obtained material. Furthermore, from a visual point of view, the obtained material appears very dark, almost black, unlike the other brown-coloured materials. In order to try to obtain a greater quantity of material, the reaction was repeated in double concentration (50 mL of solvent instead of 100 mL) but the result was similar to the previous one (entry 7).

Reactions with silane **E**, carried out under the previous different conditions, gave the corresponding materials with similar TGA (entries 8–10). Primary amine-based materials **A2** and **E2** (entries 3 and 8) prepared under the same conditions showed the same silane loading. Material **AD6.5** displayed a total silane content similar to primary amine-based materials (entry 11). However, from TGA it is not possible to ascertain to relative amount of the two silanes in the material. Imidazolium-based materials gave similar total silane loadings except, as expected, in the case of **AF1.10** which was prepared using a low amount of silane **A** (entries 12–15).

¹³C and ²⁹Si cross polarisation magic angle spinning (CP-MAS) NMR spectra of prepared materials are reported in the ESI section (Figure S2). In Figure 2 are reported the ¹³C NMR spectra of **A0** (a), **A2** (b), **D2d** (c), and **E2d** (d). The ¹³C CP-MAS NMR spectra clearly show signals related to the propyl chain bearing the corresponding amino moiety (Figure 2). In the case of **D2d**, signals of the *N,N*-dimethylaminopropyl chain is present while, in the case of **E2d** it is present the signal at ca. -1 ppm which is related to the methyl linked to silicon. The very large signal patterns, starting from ca. 110 ppm to ca. 180 ppm are

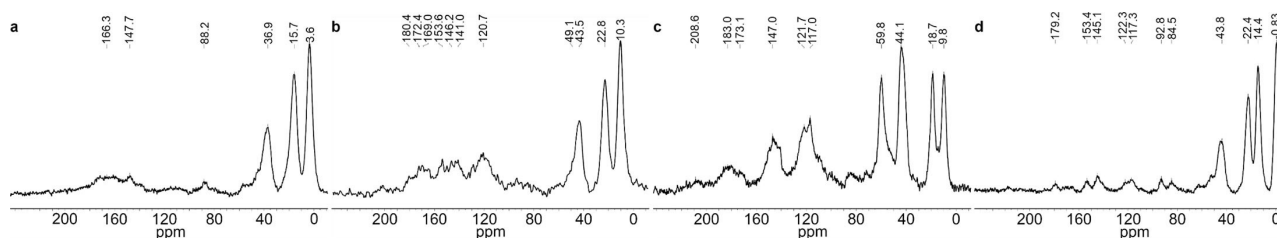


Figure 2. ¹³C MAS NMR spectra of **A0** (a), **A2** (b), **D2d** (c), and **E2d** (d).

attributable to the complex catechol-based structures, comprising both aromatic catechol rings and o-quinones-based structures. In the ^{13}C CP-MAS NMR spectrum of **A0** the intensity of aromatic signals is low due to the large presence of the silica moiety whereas, in the case of **D2d** the intensity of aromatic signals is higher because of the reduced presence of the silica-based moiety.

In Figure 3 ^{29}Si CP-MAS NMR spectra of materials **A0** (a), **A2** (b), **D2d** (c), and **E2d** (d) are reported. Such spectra display signals attributable mainly to T3 species $\text{RSi}(\text{OSi})_3$ and, especially in the case of **D2d**, T2 species which can be ascribed to $\text{RSi}(\text{OH})(\text{OSi})_2$, $\text{RSi}(\text{OMe})(\text{OSi})_2$ and/or $\text{RSi}(\text{OPh})(\text{OSi})_2$ ^[13] contributions. ^{29}Si NMR spectra of **E2d** shows a signal at ca. -23 ppm due to the D2 $\text{R}_2\text{Si}(\text{OSi})_2$ species with a small shoulder due to the D1 $\text{R}_2\text{Si}(\text{OH})(\text{OSi})$ species. In the case of **A0**, peaks at around 100 – 108 ppm are observable. These signals could be related to Q systems which presence could be due to dealkylation at the silicon atom that has occurred in some extent to give the $\text{Si}(\text{OSi})_4$ and $\text{Si}(\text{OSi})_3\text{OH}$ systems. Dealkylation of silicon atom in the presence of catechol has been reported.^[14] It should be noted that **A0** has been obtained in the absence of the oxidizing agent then, catechol was present in large amount when the silane was added. In Figure 4 ^{13}C and ^{29}Si MAS NMR spectra of **AD6.5** and **AG6.5** are reported. In the case of **AD6.5**, signals due the presence of the two different aminopropyl chains are present. Also in the case of **AG6.5**, signals due to the presence of the aminopropyl chain and propyl-3-(1-methylimidazolium) moiety are present as well as signals due to the imidazolium ring. ^{29}Si CP-MAS NMR spectra of the latter materials again show signals attributable mainly to T3 and T2 species.

The XPS survey spectra for the prepared materials and spectra of N1s, C1s and O1s are reported in Figures S3–12 (ESI). In Figure 5, XPS spectra of **D2d** are reported, as an example. The survey XPS spectrum of **D2d** (Figure 5a) revealed the presence of O, N and C atoms with the corresponding peaks at

532.6 eV, 402.1 eV and 285.1 eV, respectively. Furthermore, representative peaks for the $\text{Si}2s$ and $\text{Si}2p$ are also observed, due to the presence of the silane moieties.

The N1s spectrum (Figure 5b) was deconvoluted into two peaks centered at 399.4 , and 402.1 eV corresponding to $-\text{NH}_2$ and $-\text{NH}_3^+$, respectively. The XPS spectrum of C1s (Figure 5c) was deconvoluted into three peaks corresponding sp^2 ($\text{C}=\text{C}$) at 284.7 eV, $\text{C}-\text{OH}/\text{C}-\text{N}$ at 286.1 eV, as well as $\text{C}=\text{O}$ at 288.3 eV. Contribution of possible peak at ca. 283 eV due to $\text{C}-\text{Si}$ is not clearly visible. The O1s spectrum (Figure 5d) also confirmed the coexistence of the aforementioned species (deconvoluted into three peaks at 530.9 eV, 532.2 eV and 533.4 eV corresponding to $\text{C}=\text{O}$, $\text{O}-\text{Si}$ and $\text{C}-\text{OH}$, respectively). These spectra clearly show the existence of some expected functional groups, such as amine, carbonyl and hydroxyl moieties.^[4d,7c,e,h,15] XPS spectra and deconvolution analysis of other materials (see ESI, Tables S1–3) show an almost identical deconvolution pattern for all the materials prepared.

In particular, it is worthy to discuss the N1s band in the XPS spectra of materials (see SI and Table 2). In some cases, two peaks can be fitted with binding energies at ca. 399 and 401 eV. In the case of **B2** and **E2d** only one peak was present. The lower binding energy nitrogen peak is attributed to free amines, while the higher binding energy peak could be related to protonated and H-bonded amines.

Hydrogen-bonding interactions may take place between the amine groups and neighbouring surface phenol groups or silanol groups. This situation resembles the acid-base reaction to yield the protonated species reported in the case of nitrogen abstraction of a proton from a silanol group reported in the case of aminoalkoxysilane-based materials.^[16] A comparison of the two peaks ratio, can give information about the basicity of the surface bound amine groups. Based on the N1s area ratios, basicity in the dry state follows the trend diamine $< \text{NH}_2 < \text{N}$ -methyl $< \text{N,N}$ -dimethyl, consistent with vapour phase basicity that follows the same trend.

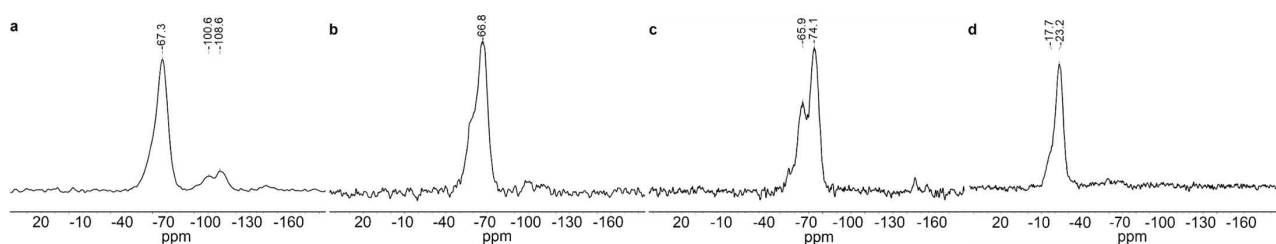


Figure 3. ^{29}Si NMR spectra of **A0** (a), **A2** (b), **D2d** (c), and **E2d** (d).

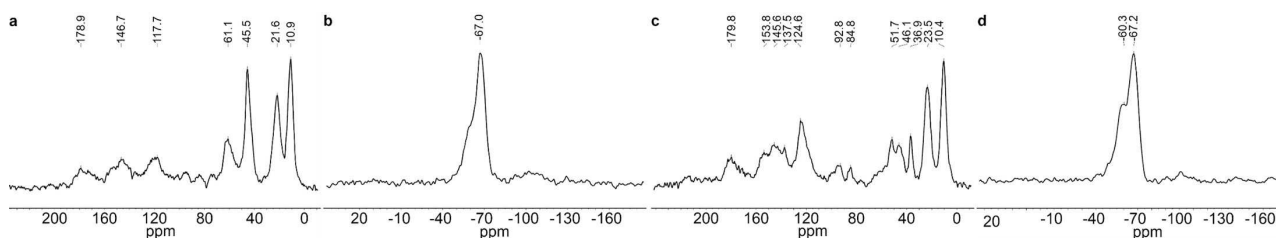


Figure 4. ^{13}C and ^{29}Si MAS NMR spectra of **AD6.5** (a) and (b), and **AG6.5** (c) and (d).

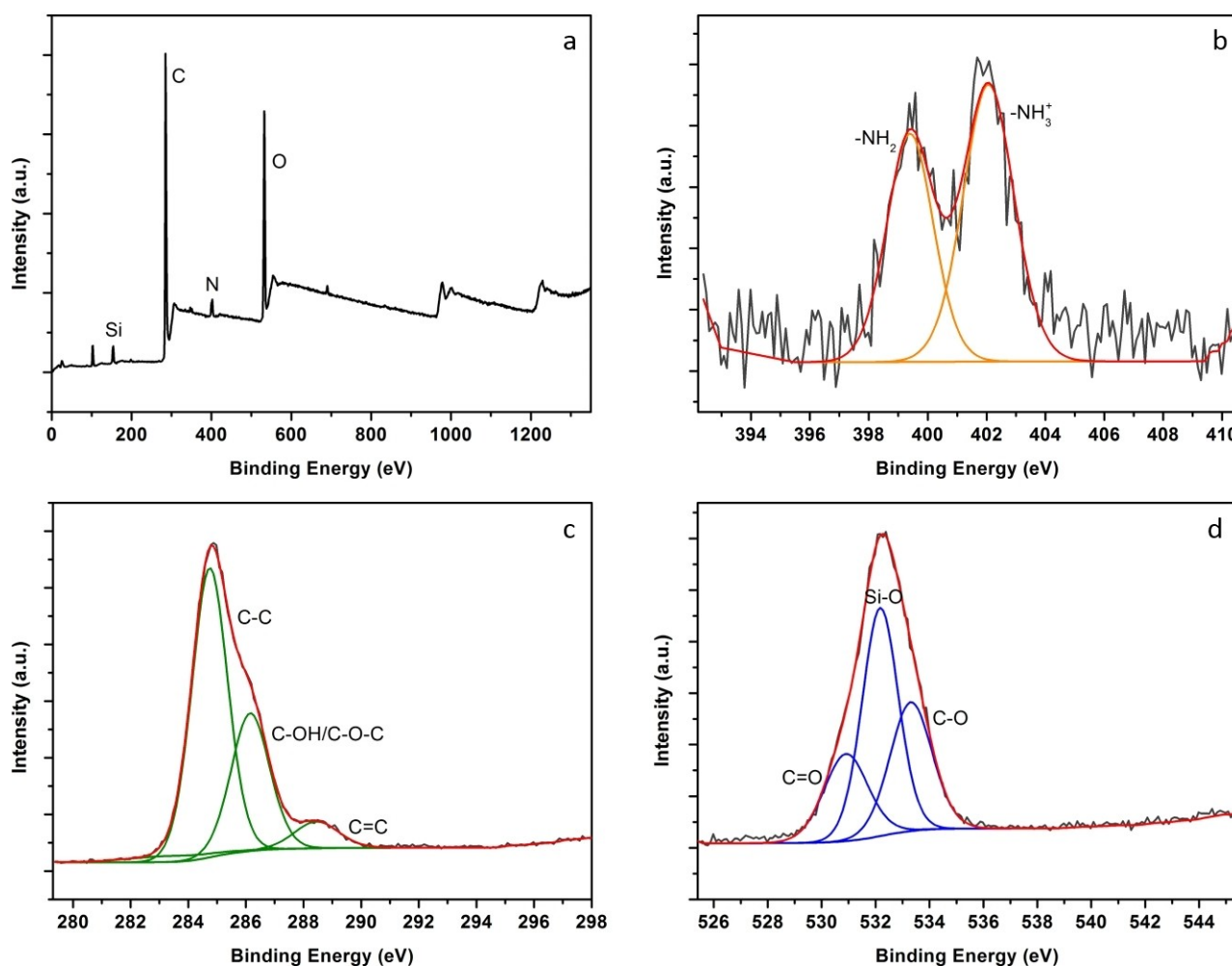


Figure 5. (a) XPS survey of D2d; (b) deconvoluted N1s spectrum; (c) deconvoluted C1s spectrum and (d) deconvoluted O1s spectrum.

Table 2. Binding energies and atomic percentage of deconvoluted peaks of N1s XPS spectra.			
Entry	Material	C–N eV [atomic %]	C–NH ⁺ eV [atomic %]
1	A0	399.5 (87%)	401.7 (13%)
2	A1	399.4 (90%)	401.7 (10%)
3	A2	399.5 (85%)	401.8 (15%)
4	B2	399.6 (100%)	–
5	C2	399.5 (65%)	401.5 (35%)
6	D2d	399.4 (42%)	402.1 (58%)
7	E2d	399.7 (100%)	–
8	AD6.5	399.5 (79%)	402.2 (21%)
9	AF6.5	399.6 (65%)	401.8 (35%)
10	AG6.5	399.6 (65%)	401.8 (35%)
11	EH6.5	399.7 (69%)	401.7 (31%)

Comparison within primary amine-based materials (A0, A1, A2, Table 2, entries 1–3) shows a similar basicity. The presence of only one peak due to the free amine in the case of E2d (entry 7) is interesting and could be attributed to the different nature of the material, being it more hydrophobic than the other materials. AD6.5 (entry 8) possessing primary and tertiary amine moieties shows a similar behaviour to A2 whereas the

presence of the second peak the case of materials prepared with imidazolium-based silanes can be also due to the presence of the imidazolium moiety (entries 9–11).

The FT-IR spectra of prepared materials (Figure S13) were similar showing a large and broad peak centered at ca. 3350 cm⁻¹ due to the presence of amine and hydroxyl groups as well as bonded and free water molecules. The peak at ca. 1600 cm⁻¹ can be ascribed to the stretching vibration of C=O whereas the C=C stretching vibration of the aromatic rings generated the peak at ca. 1590 cm⁻¹. Peaks centered at ca. 1111 cm⁻¹ and 1020 cm⁻¹ were assigned to the symmetric stretching vibration modes of C–O and to the Si–O–Si stretching vibrations, respectively whereas the sharp peak at 1260 cm⁻¹ in E2d and EH6.5 is due to the Si–CH₃ stretching vibration.

SEM analysis of selected materials (Figures S14–17) showed different morphologies depending on the silane used. Regular round-shaped nanostructures, typical of polydopamine-like materials were observed in the case of primary amine-based silane materials whereas different morphology was observed for the tertiary amine-based silane material. EDX mapping (Figur-

es S18–20) showed a homogeneous distribution of silicon and nitrogen atoms in the matrix.

As a further step in the characterisation investigation, we decided to determine the pH_{PZC} of selected materials (Figure S21). This value may help to shed some light in the deprotonation-protonation characteristics of the surface of a material since it represents the point at which the surface basic (or acidic) functional groups no longer contribute to the pH value of the solution.^[17] In Table 3 pH_{PZC} values for selected representative materials are reported. Values of pH_{PZC} were similar for **A2**, **C2** and **D2d** irrespective for different amino functionalities and decreasing loadings. Lower values were found in the case of **A0** and **E2d** indicating that, despite the presence of the primary amino group as for **A2**, such materials behaved differently. **AD6.5**, possessing two amino functionalities, gave a higher pH_{PZC} value. Although not directly correlatable since a comparison between dry state (XPS analysis) and aqueous conditions (pH_{PZC}) is not consequential, the lower basicity of **E2d** resemble what we observed with N1s analysis in XPS with respect to the other materials.

The textural properties of the materials were investigated via nitrogen physisorption analysis. Figures S22–27 show the reversible isotherms characterised by a sharp increase of the adsorbed volume at a relative pressure close to 1. According to IUPAC classification, the described features can be related to type II isotherm, consistent with macroporous absorbents. The specific surface area (SSA) of the solids was calculated using the Brunauer-Emmett-Teller (BET) method ($0.05 < P/P_0 < 0.3$). The values reported in Table 4 show that the solids display a low SSA in the range of 4–63 m^2g^{-1} .

Based on the above characterisation data, the obtained hybrid materials contain large domains of aminopropyl moieties as well as aromatic/quinone moieties.

The first step of the synthesis involves the fast oxidation of catechol to *o*-quinone. Under such conditions, *o*-quinone can react via reverse dismutation with catechol, to give highly reactive semi-quinone radicals that can couple to form diaryl compounds which can be further transformed/oxidised.^[18] In

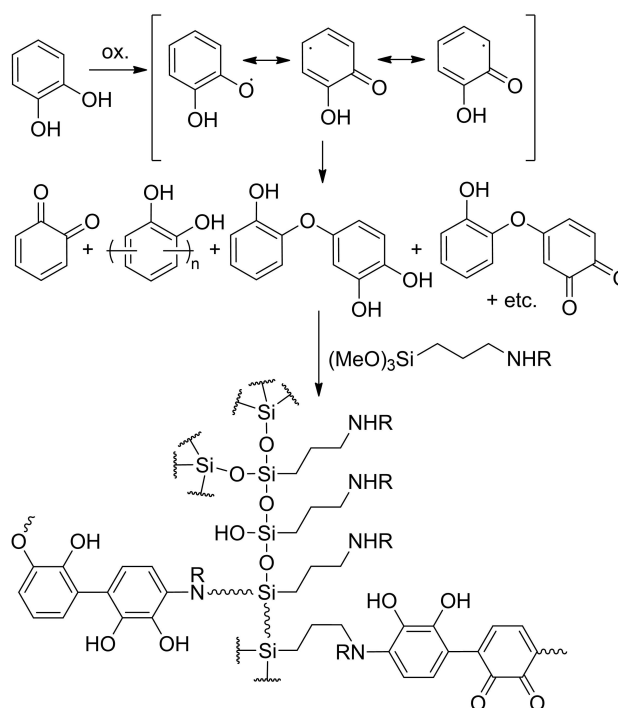
Entry	Material	pH_{PZC}
1	A0	7.4
2	A2	8.7
3	C2	8.3
4	D2d	8.8
5	E2d	6.6
6	AD6.5	9.7

Entry	Material	SSA [m^2g^{-1}]
1	A0	4
2	A1	13
3	A2	63
4	B2	24
5	C2	16
6	D2d	5
7	E2d	10

the second step, the main reactions are based on Michael-type addition with only a small fraction of products formed via Schiff base reactions^[5] and hydrolysis and condensation of the trimethoxysilyl moiety (Scheme 1). The structures reported in Scheme 1 and Figure 6 (vide infra) do not correspond to the exact nature of the materials and exact composition of phenolic and amine moieties present in each material but are a tentative way to represent them.

With the aim to explore the availability of amino moieties on the surface of the synthesised materials, Knoevenagel reactions between ethyl cyanoacetate, as a substrate containing α -acid hydrogens, and 3-methoxybenzaldehyde were carried out. Catalytic tests were run using 10 mg of each material and 1 mmol of each reactant solubilised in 1 mL of ethanol. In selected cases, reactions were also carried out in toluene and in water.

Material **A0** gave a very low yield (entry 1), despite showing the highest loading in silane, which could also indicate a high



Scheme 1. Tentative structure based on characterisation data (see discussion).

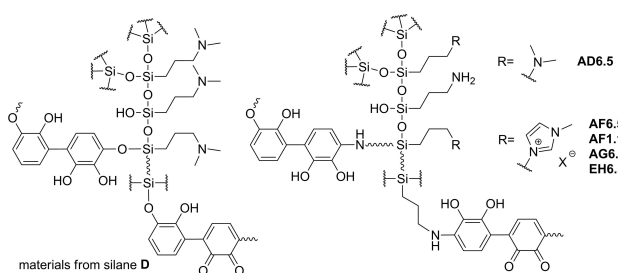


Figure 6. Tentative structure of materials based on silane D and from two silanes.

load in amino groups, given that the amino function is present in the starting silane. This result could be an indication of the low availability of the amino functions. In addition, the ^1H NMR spectrum showed the presence of the corresponding diethyl acetal (ca. 22%) that removes the starting aldehyde to the Knoevenagel reaction. Indeed, a higher yield was afforded in water (entry 2). From XPS data (see Table S1, entry 1) **A0** appears to be the material having the lowest N/Si atomic ratio, then indicating the lowest amine availability on the surface. The oxidation of catechol with KIO_4 provided materials with a slightly higher catalytic activity in ethanol (entries 3 and 5). In the case of **A2**, reactions were also carried out in toluene and in water showing a dependence of the yield on the polarity of the solvent employed (entries 4–6). The higher yield observed with diamine (entry 7) is explained by the presence of two amino functions, one primary and one secondary which consequently leads to a higher catalytic loading. The use of the material containing only a secondary amino function showed, indeed, an intermediate yield (entry 8).

Results observed with the two materials having the tertiary amino function are very interesting (entries 9–12). Although they possess a lower loading, the observed yields were higher than the previous ones. This could also be due to the greater presence of tertiary amino groups available for catalysis, since no Michael's addition can take place. The good N/Si atomic ratio displayed at XPS could indicate such availability (Table S1). No difference was observed when water was used instead of ethanol (entries 10 and 11) whereas very low yield was observed in toluene (entry 9).

High yields were also reached with materials **E2** and **E2d** having the primary amino function. These materials were prepared using the corresponding dimethoxymethyl silane. It should be noted that materials **A2** and **E2**, have the same silica loading (6.1 mmol/g) but quite different catalytic activity (entries 5 and 13). Probably, the two materials possess a different hydrophobicity due to the presence of the methylsilane moiety in **E2** as demonstrated by the different water content (see Table 1). Catalyst **E2d** was also tested in toluene, ethanol and water (entries 14–16). Again, yield in toluene was the lowest while the same yield was observed in the polar solvents. Material **E1d** prepared with lower amount of oxidizing agent gave slightly higher yields (entries 17 and 18) as in the case of entry 3.

Another comparison could be made between **A1** and **E2d**. Even if the experimental conditions for their synthesis were different, these primary amino-based materials showed similar silane loading, SSA, N/Si atomic ratio and N/NH $^+$ ratio from XPS. Again, the great difference in activity could be ascribed to the different hydrophobicity as seen from the different amount of water in the TGA.

Catalyst **AD6.5** gave the highest yield in water. This result is in agreement with the higher pH_{PZC} for **AD6.5**. Imidazolium-based materials gave also interesting results showing that such moiety had an important role. Indeed, **AF6.5** gave a high yield, much higher to the simple primary amine-based catalyst **A2** (entry 21 vs entry 5).

Catalyst **AF1.10** (entries 23 and 24) that displayed a low silane content (Table 1) and was prepared using a large excess of imidazolium-based silane compared to the primary amine-based one, still gave a high yield despite the much lower silane loading. The role of the imidazolium salt is highlighted by role of its anion. Indeed, when iodide was used in place of chloride a lower yield was observed. Finally, **EH6.5** which was prepared using the dimethoxymethyl corresponding silanes gave, as for **E2** and **E2d**, a higher yield when compared to **AF6.5** (entries 27, 28 vs 21, 22) and the highest yield in ethanol.

In order to investigate if the sole solvent had a role, reactions were carried out in toluene, ethanol and water without catalyst (entries 29–32). Indeed, uncatalysed reactions may take place.^[19]

It is interesting to observe that in ethanol a good yield value was obtained. As already observed by Patai, ethanol, behaves as a stronger base than water. On the other hand, water, owing to its greater solvating power and higher dielectric constant, stabilises the carbanions formed. The yield value in ethanol is higher than that obtained using **A0** and comparable to that obtained with **A1** and **A2**. In other words, **A0**, **A1** and **A2** had, practically, no catalytic effects. **A0** seems to have an inhibiting effect on the reaction probably because actually catalysed the acetal formation.

From a mechanistic standpoint, several pathways may be operative, the ion-pair mechanism, favoured by tertiary amines; a mechanism *via* carbinolamine, iminium, and enolate intermediates catalysed by secondary amines^[20] and the mechanism involving a covalent imine intermediate, favoured by primary amines.^[21] In addition, as for the role played by silanol groups,^[22] a possible role of phenolic hydroxyl groups can be also operative.

As already discussed, materials may possess different functional groups. Even using, as starting reactant, the primary aminopropyl silane, different amino functions, such as secondary amines and imine moieties, can be present in the final material. Then, different pathways can be operative in which the different functional groups can work cooperatively.^[23] On the other hand, since polar solvents aid the ion-pair mechanism by stabilizing the carbanion intermediate,^[24] it is possible a large contribution of such mechanism.

As reported above, **A0** showed a very low catalytic activity in ethanol and higher in water. The features of **A0** are a high loading of silane, but a low N/Si atomic ratio as seen from XPS which could indicate that amino functionalities are less available on the surface of the material. In addition, pH_{PZC} was lower than other materials prepared from trimethoxysilane derivatives. **A0** was the only material which has catalysed the formation of a certain amount of the diethyl acetal, removing the aldehyde from the equilibrium. The use of water in place of ethanol had a good effect since no acetal can be formed and, because of its higher polarity that stabilises the carbanions formed, effectively depressed their recombination rate with protons.

It can be easily seen that there is no correlation between pH_{PZC} values (Table 3) and catalytic activity when we compare primary amine-based materials. Despite the very low surface

area value and lower basic strength, **E2d** was the most active catalyst. This result could be ascribed, as already supposed, to its higher hydrophobicity of the solid surface due to the use of the dimethoxymethyl-based silane. As reported in the literature, primary aminoalkyl modified polysilsesquioxanes^[25] gave an increased yield with increased solvent polarity, supporting the idea of a partitioning effect due to the higher hydrophobicity of polysilsesquioxanes compared to silica materials. A similar behaviour was observed by us for the proline-catalysed asymmetric aldol reaction^[26] in which the use of water afforded higher yields in the aldol products due to partitioning effect. In our case, when reactions were carried out in toluene (Table 5, entries 4, 9 and 14), a solvent in which reactants are well dissolved, lower yields were obtained because reactants were not forced toward the surface of the catalysts. The use of water, a reaction medium in which reactants are not well dissolved, forced the latter toward the surface giving a better yield with the more hydrophobic catalyst (Table 5, entries 6 vs 16).

In the examined cases, the higher catalytic activity in ethanol than in toluene is also in agreement with the presence of other catalytic moieties on the surface that operate through the ion-pair mechanism (see ESI).^[27] The high catalytic activity of **D2** could be due to its higher basic strength. The almost no catalytic activity observed with **D2** in toluene is an indication that the ion-pair mechanism is operative with tertiary amine-based catalyst. Overall, materials displayed higher catalytic activity in water since the yield without catalyst in water was much less than in ethanol.

After these preliminary tests, we decided to test the recyclability of the most promising catalytic materials. For this procedure 20 mg of catalyst were used. The reactions were carried out in ethanol or water (1 mL) using 2 mmol of ethyl cyanoacetate and several aldehydes. At the end of each

reaction, the product was separated from the reaction mixture and analysed by ¹H-NMR, while the catalyst, recovered by centrifugation, after being dried, was used for the next cycle without any reactivating procedure. First, we investigated catalysts prepared using a single silane.

The first recycling study was performed using the diamine-based catalyst **B2** using 2,4-dimethoxybenzaldehyde. After a reaction time of 5 h, a yield of 88% was observed. The second cycle gave a lower yield (74%). In addition to such decreased activity, the material was not easily recovered as a loss of about 40% by weight was found after only two cycles. Then, no subsequent cycles were carried out. The second catalytic material investigated was **C2**. By using the same 2,4-dimethoxybenzaldehyde and a reaction time of 5 h the yield was 54% which decreased in the second cycle (43%). Given these results, it was decided not to carry out any further reaction cycles.

Table 6 shows the ten cycles made with **D2**. For each benzaldehyde, the corresponding reaction without catalyst was carried out for comparison (Table 6, footnote). Three different substrates were used. It can be observed that yield values constantly decreased after the first five cycles in which 2,4-dimethoxybenzaldehyde was used. The following three cycles (from 6 to 8), lasting 1 hour, were carried out using 4-nitrobenzaldehyde; the obtained results showed a total yield of the aldehyde in line with the greater reactivity of the aldehyde. At this point the ninth cycle was run out again with the less reactive 2,4-dimethoxybenzaldehyde to verify the variation of the catalytic activity of the material after eight cycles. A further decrease in catalytic activity was observed. In the tenth cycle 4-bromobenzaldehyde was used giving a yield of 83%.

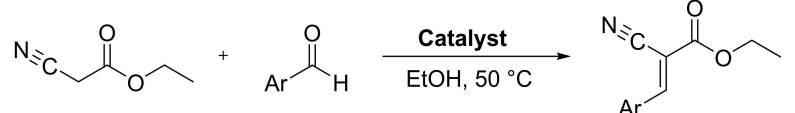
In Table 6 are also reported recycling studies with **D2d**. Also in this case, catalyst **D2d** was easily separated from the reaction mixture at the end of each cycle. Yield values, relating to 2,4-

Table 5. Knoevenagel reaction between ethyl cyanoacetate and 3-methoxybenzaldehyde.^[a]

Entry	Catalyst	Solvent	Yield [%]	Entry	Catalyst	Solvent	Yield [%]
1	A0	EtOH	6 ^[b]	17	E1d	EtOH	84 ^[c]
2	A0	H ₂ O	34	18	E1d	H ₂ O	80
3	A1	EtOH	33	19	AD6.5	EtOH	75
4	A2	Toluene	19	20	AD6.5	H ₂ O	93
5	A2	EtOH	25	21	AF6.5	EtOH	80
6	A2	H ₂ O	42	22	AF6.5	H ₂ O	69
7	B2	EtOH	76	23	AF1.10	EtOH	75
8	C2	EtOH	56	24	AF1.10	H ₂ O	64
9	D2	Toluene	6	25	AG6.5	EtOH	59
10	D2	EtOH	82	26	AG6.5	H ₂ O	62
11	D2	H ₂ O	83	27	EG6.5	EtOH	92
12	D2d	EtOH	82	28	EH6.5	H ₂ O	87
13	E2	EtOH	72	29	No catalyst	Toluene	< 5
14	E2d	Toluene	34	30	No catalyst	EtOH	30
15	E2d	EtOH	77 ^[c]	31	No catalyst	H ₂ O	8
16	E2d	H ₂ O	75	32	No catalyst	–	< 5

[a] Reaction conditions: catalyst (10 mg), 3-methoxybenzaldehyde (1 mmol), ethyl cyanoacetate (1 mmol), solvent (1 mL). [b] Diethyl acetal (22% from ¹H NMR of the crude reaction mixture). [c] Traces of diethyl acetal.

Table 6. Recycling studies with **D2**, **D2d** and **E2d**.^[a]



Entry	Cycle	Ar	Time [h]	Catalyst D2 Yield [%]	Catalyst D2d Yield [%]	Catalyst E2d Yield [%]
1	1	2,4-diMeO	5	91 ^[b]	91 ^[b]	97 ^[b]
2	2	2,4-diMeO	5	88	95	97
3	3	2,4-diMeO	5	79	63	97
4	4	2,4-diMeO	5	69	75	97
5	5	2,4-diMeO	5	54	44	88
6	6	4-NO ₂	1	> 99 ^[c]	> 99 ^[c]	98 ^[c]
7	7	4-NO ₂	1	> 99	> 99	97
8	8	4-NO ₂	1	> 99	> 99	97
9	9	2,4-diMeO	5	32	51	98
10	10	4-Br	2.5	83 ^[d,e]	91 ^[d,e]	43 ^[d,f]

[a] Reaction conditions: catalyst (20 mg), aldehyde (2 mmol), ethyl cyanoacetate (2 mmol), ethanol (1 mL). [b] Yield without catalyst: 20%. [c] Yield without catalyst: < 5%. [d] Yield without catalyst: 32%. [e] Yield with fresh catalyst: 93%. [f] Yield with fresh catalyst: 97%.

dimethoxybenzaldehyde, show a fluctuating trend although decreasing between the first and fifth cycle. The ninth cycle shows a higher yield than the fifth. Yields relating to 4-nitrobenzaldehyde were quantitative. The value obtained in the tenth cycle, where 4-bromobenzaldehyde was used, showed a high yield, if compared to the yield obtained using the same aldehyde and fresh catalyst in its first cycle (93%).

Another set of recycling investigation was carried out with catalyst **E2d** (Table 6). The results obtained for the first four cycles show very high yield values; in the fifth cycle, where 2,4-dimethoxybenzaldehyde was still used, a slight decrease was observed. The cycles where 4-nitrobenzaldehyde was used (from 6 to 8) show also high and constant yield values. The ninth cycle gave again a high yield. The value reported in the table referring to 4-bromobenzaldehyde showed a sudden decrease in the catalytic performance of the material, which is confirmed by the comparison with the yield obtained with **E2d** in the first cycle using 4-bromobenzaldehyde which was 97%.

Reused catalysts were analysed by TGA after 10 cycles and results compared with the fresh ones (Table 7). Catalyst **D2** was highly stable as well as catalyst **D2d**, whereas a small loss was observed in the case of **E2d** that, actually, gave a much lower yield in the 10th cycle. It must be considered that the lower the residue, the lower the amino counterpart.

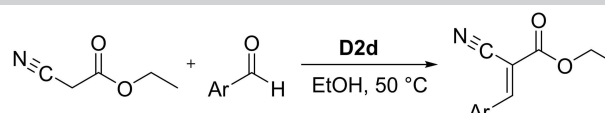
Table 7. TGA and loading of fresh and reused catalysts.^[a]

Entry	Catalyst	TGA residue [%]		Loading [mmol/g]	
		Fresh	After reuse	Fresh	After reuse
1	D2	21.4	20.6	3.6	3.4
2	D2d	21.3	21.1	3.6	3.5
3	E2d	39.4	31.0	6.6	5.2
4	AD6.5	39.8	26.8	6.6	4.5
5	EH6.5	33.7	27.7	5.6	4.6

[a] TGA of **D2**, **D2d**, **E2d** after 10 cycles; TGA of **AD6.5**, **EH6.5** after 8 cycles.

We carried out further recycling tests on **D2d** (Table 8). In a first set, 4-chlorobenzaldehyde was used up to five cycles showing constant yields in the first four cycles and a slight decrease in the fifth. Then, quantitative yields were observed in the next two cycles with 4-nitrobenzaldehyde. In the subsequent cycle, again with 4-chlorobenzaldehyde, no decrease in activity was observed compared to the fifth cycle (entries 1–8). The recovered catalyst in entry 7 was used again with 4-chlorobenzaldehyde giving the same result in entry 5. In a second set of recycling reactions still good results were obtained (entries 9–12). Both set of recycling confirmed a good level of recyclability of the material. Then, we used catalysts **AD6.5** and **EH6.5** for recycling studies (Table 9). **AD6.5** was tested in ethanol and in water, due to its excellent result in this medium (see Table 5). **EH6.5** was used in ethanol. Better performances were observed using **EH6.5**. Thermogravimetric

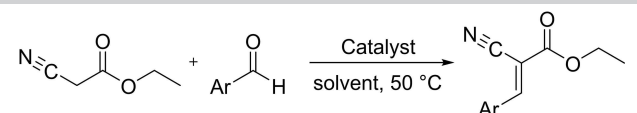
Table 8. Recycling studies with **D2d**.^[a]



Entry	Cycle	Ar	Time [h]	Yield [%]
1	1	4-Cl	2.5	95 ^[b]
2	2	4-Cl	2.5	93
3	3	4-Cl	2.5	94
4	4	4-Cl	2.5	92
5	5	4-Cl	2.5	82
6	6	4-NO ₂	1	> 99
7	7	4-NO ₂	1	> 99
8	8	4-Cl	2.5	83
9	1	2-NO ₂	1	95 ^[c]
10	2	4-Br–3-OMe	1.5	95 ^[d]
11	3	Bithiophenyl	4	84 ^[e]
12	4	4-Br	1.5	71 ^[f]

[a] Reaction conditions: catalyst (20 mg), aldehyde (2 mmol), ethyl cyanoacetate (2 mmol), ethanol (1 mL). [b] Yield without catalyst: < 5%. [c] Yield without catalyst: 85%. [d] Yield without catalyst: < 5%. [e] Yield without catalyst: 7%. [f] Yield without catalyst: 14%.

Table 9. Recycling studies with AD6.5 and EH6.5.^[a]



Entry	Cycle	Ar	Time [h]	Catalyst AD6.5 ^[b] Yield [%]	Catalyst AD6.5 ^[c] Yield [%]	Catalyst EH6.5 ^[b] Yield [%]
1	1	2,4-diMeO	5	99 ^[d]	99 ^[d]	99 ^[d]
2	2	2,4-diMeO	5	85	98	95
3	3	2,4-diMeO	5	82	94	95
4	4	2,4-diMeO	5	88	83	99
5	5	4-NO ₂	1	> 99 ^[e]	> 99 ^[e]	> 99 ^[e]
6	6	4-NO ₂	1	> 99	> 99	> 99
7	7	4-Br	2.5	73 ^[f]	79 ^[f]	89 ^[f]
8	8	4-Cl	2.5	55 ^[g]	45 ^[g]	45 ^[g]

[a] Reaction conditions: catalyst (20 mg), aldehyde (2 mmol), ethyl cyanoacetate (2 mmol), ethanol (1 mL). [b] Solvent: ethanol. [c] Solvent: water. [d] Yield without catalyst: 20%. [e] Yield without catalyst: < 5%. [f] Yield without catalyst: 32%. [g] Yield without catalyst: < 5%.

analysis after 8 cycles evidenced a certain loss both for AD6.5 and EH6.5 (Table 2, entries 4 and 5).

Conclusion

By mimicking the polydopamine chemistry, we prepared a set of hybrid organic-inorganic materials in a one-pot procedure under mild conditions. This procedure is based on the use of catechol and KIO₄ as oxidizing agent in conjunction with 3-aminopropyl- or substituted 3-aminopropyl- or 3-methylimidazolium-1-trimethoxypropylsilane. The first step of the synthesis involves the fast oxidation of catechol to *o*-quinone giving a complex mixture of aryl compounds which may undergo mainly Michael-type addition with primary or secondary aminopropyltrimethoxysilanes followed by hydrolysis and condensation of the trimethoxysilyl moiety. Characterisation of the hybrid materials indicated the presence of several functional groups. Then, Knoevenagel reaction between ethyl cyanoacetate and several benzaldehydes was chosen as good probe to investigate the availability of functional groups on the surface. In such a way it was possible to identify the best reaction conditions and the use of the proper aminopropylsilanes for the obtainment of the most active catalytic materials. In particular, materials D2d and AD6.5 possessing a tertiary amine gave good results. Materials based only on primary amine gave no good results unless they were prepared using a dimethoxymethyl-based silane. In the latter case, the enhanced hydrophobicity could be the reason for the increased catalytic activity. Probably, a similar effect was operative in the case of EH6.5. Such simple procedure could be of interest for the development of new hybrid organic-inorganic multifunctional materials for several purposes.

Experimental Section

Spectroscopic and Analytical Methods

Chemicals and solvents were purchased from commercial suppliers to be used without further purification. Thermogravimetric analysis (TGA) measurements were carried out under oxygen flow from 100 to 1000 °C with a heating rate of 10 °C min⁻¹ in a Mettler Toledo TGA STAR Combustion chemical analysis was performed on a PerkinElmer 2400 Series II Elemental Analyzer System. Nitrogen adsorption-desorption analysis was performed at 77 K by using a volumetric adsorption analyzer (Micromeritics ASAP 2420). Before the analysis, the sample was pre-treated at 150 °C for 16 h under reduced pressure (0.1 mbar). The BET method was applied in the $p/p_0 = 0.05-0.30$ range to calculate the specific surface area. X-ray photoelectron spectroscopy (XPS) analyses were performed with a Thermo Fisher ESCALAB 250Xi instrument equipped with a monochromatic Al K α X-ray source (1486.6 eV) and a hemispherical deflector analyzer (SDA) working at constant pass energy (CAE) allowing to obtain a constant energy resolution on the whole spectrum. The experiments were carried out using a 200 μ m diameter X-ray spot. The charge neutralisation of the sample was achieved with a flood gun using low energy electrons and argon ions. The pressure in the analysis chamber was in the range of 10⁻⁸ Torr during data collection. Survey spectra were recorded with a 150 eV pass energy, whereas high-resolution individual spectra were collected with a 20 eV pass energy. Analyses of the peaks were performed with the software Thermo Avantage, based on the non-linear squares fitting program using a weighted sum of Lorentzian and Gaussian component curves after background subtraction according to Shirley and Sherwood.^[28] Full width at half maximum (FWHM) values were fixed for all the signals. Solid state CP-MAS ¹³C-NMR spectra were recorded at room temperature, on a Jeol ECZ-R 600 MHz spectrometer operating at 14.1 T, using a contact time of 2 ms, a spinning rate of 8 KHz and a automas probe of 3.2 mm. CP-MAS ²⁹Si-NMR spectra were recorded at room temperature, on a Jeol ECZ-R 600 MHz Spectrometer operating at 14.1 T, using a contact time of 2 ms, a spinning rate of 8 KHz and a automas probe of 3.2 mm. Liquid state ¹H NMR spectra were collected on a Bruker 300 MHz spectrometer. IR spectra (KBr disk) were recorded on an Agilent Technologies Cary 630 FT-IR spectrometer. Specimens for these measurements were prepared by mixing 1 mg of the sample powder with 100 mg of KBr. The pH of point of zero charge (pH_{PZC}) was determined as follows.^[29] The pH of a series of 20 mL 0.01 M NaCl solutions was adjusted to a value between 4 and 10 by adding HCl 0.1 M or NaOH 0.1 M solution in closed Erlenmeyer flasks. Before adjusting the pH, all solutions were degassed by purging Ar gas to remove dissolved CO₂. The pH of these solutions was recorded as the initial pHs (pH_i). Then, 0.1 g of material was added and the final pH (pH_f) was measured after 24 h. The plots of both pH_f vs pH_i and pH_f vs pH_i gave the pH_{PZC} value as the intersection of the curves. Scanning electron microscopy images were recorded with a JEOL 7500F coupled with an energy-dispersive X-ray detector. The Knoevenagel reaction products are known molecules and their spectroscopic and analytical data correspond to those reported in the literature. (E)-ethyl 3-(4-bromo-3-methoxyphenyl)-2-cyanoacrylate (Table 8, entry 10) has not been reported in the literature.

Synthesis of hybrid materials (Table 1)

General protocol: catechol (4.36 mmol) was dissolved into a buffer solution (KHCO₃/K₂CO₃, pH 9, 10 mM, 100 mL or 50 mL) under magnetic stirring at room temperature. Then, KIO₄ (0.5 or 0.25 eq) was added to the solution. The above mixture was stirred at room temperature for 2.5 h. After this period, the amino-based organo-

silane (10 mmol) was added. The reaction mixture was stirred for 18 h at 70 °C. The brown solid was filtered and washed with water, ethanol, methanol and diethyl ether. The obtained material was dried at 60 °C under reduced pressure.

General procedure for the Knoevenagel condensation between 3-methoxybenzaldehyde and ethyl cyanoacetate

The catalytic tests were run into a 10 mL a glass vial with screw cap in which 10 mg of catalytic material, 3-methoxybenzaldehyde (1 mmol), ethyl cyanoacetate (1 mmol), and ethanol (1 mL) were placed. The reaction mixture was sonicated for a short time and heated at 50 °C under stirring for 5 h. Then, the reaction mixture was allowed to cool down to room temperature, diluted with dichloromethane and filtered for catalyst removal. The filtrate was evaporated under vacuum at room temperature. The residue was weighted and analysed by ¹H NMR spectroscopy then passed through a short pad of silica gel.

General recycling procedure for the Knoevenagel condensation

The recycling tests were run into a 10 mL a glass vial with screw cap in which 20 mg of catalytic material, the aldehyde (2 mmol), ethyl cyanoacetate (2 mmol), and ethanol (1 mL) were placed. The reaction mixture was sonicated for a short time and heated at 50 °C under stirring for a given time. Then, the reaction mixture was allowed to cool down to room temperature, diluted by addition of dichloromethane/Et₂O 5:1 (v/v), sonicated for several minutes and centrifuged at 4000 rpm for 8 min. The supernatant was recovered and the washing procedure was repeated twice with dichloromethane/Et₂O 1:1 (v/v) and finally with Et₂O. The recovered catalyst was dried at 50 °C and then reused. The collected supernatants were evaporated under vacuum at 40 °C and the residue was weighted and analysed by ¹H NMR spectroscopy.

(E)-ethyl 3-(4-bromo-3-methoxyphenyl)-2-cyanoacrylate (Table 8, entry 10).

White powder. Yield: 95%; mp 128–130 °C; ¹H NMR (300 MHz, CDCl₃): δ (ppm) 8.19 (s, 1H), 7.80–7.55 (m, 2H), 7.32 (dd, *J* = 8.2, 1.9 Hz, 1H), 4.40 (q, *J* = 7.1 Hz, 2H), 3.99 (s, 3H), 1.42 (t, *J* = 7.1 Hz, 3H); ¹³C NMR (75 MHz, CDCl₃): δ 162.25, 156.45, 153.87, 134.06, 131.77, 125.41, 118.06, 115.49, 112.18, 103.44, 62.86, 56.42, 14.15. HRMS (ESI-TOF) *m/z*: [M + Na]⁺ + calcd for C₁₃H₁₂BrNO₃Na⁺, 331.9893; found, 331.9890. FT IR (film): 3110, 3092, 2994, 2971, 2947, 2919, 2220, 1729, 1607, 1581, 1464, 1409, 1296, 1248, 1176, 1091, 1044, 1018, 850, 813, 759.

Acknowledgements

This work was carried out in the frame of the PRIN2017-2017YJMPZN project. L. Soumoy thanks the FNRS for the financial support in the context of her FRIA PhD grant. Open Access Funding provided by Università degli Studi di Palermo within the CRUI-CARE Agreement.

Conflict of Interest

The authors declare no conflict of interest.

Keywords: Dopamines · Heterogeneous catalysis · Immobilization · Silanes · Supported catalysts

- [1] a) U. Díaz, D. Brunel, A. Corma, *Chem. Soc. Rev.* **2013**, *42*, 4083–4097; b) A. Puglisi, M. Benaglia, R. Annunziata, V. Chiroli, R. Porta, A. Gervasini, *J. Org. Chem.* **2013**, *78*, 11326–11334; c) A. M. Salvo, F. Giacalone, M. Gruttadauria, *Molecules* **2016**, *21*; d) X. Liu, B. Tang, J. Long, W. Zhang, X. Liu, Z. Mirza, *Sci. Bull.* **2018**, *63*, 502–524.
- [2] a) J. Liebscher, *Eur. J. Org. Chem.* **2019**, *2019*, 4976–4994; b) M. d'Ischia, A. Napolitano, A. Pezzella, P. Meredith, T. Sarna, *Angew. Chem. Int. Ed.* **2009**, *48*, 3914–3921; *Angew. Chem.* **2009**, *121*, 3972–3979; c) M. d'Ischia, K. Wakamatsu, A. Napolitano, S. Briganti, J.-C. Garcia-Borrón, D. Kovacs, P. Meredith, A. Pezzella, M. Picardo, T. Sarna, J. D. Simon, S. Ito, *Pigm. Cell Res.* **2013**, *26*, 616–633; d) M. d'Ischia, K. Wakamatsu, F. Cicoira, E. Di Mauro, J. C. Garcia-Borrón, S. Commo, I. Galván, G. Ghanem, K. Kenzo, P. Meredith, A. Pezzella, C. Santato, T. Sarna, J. D. Simon, L. Zecca, F. A. Zucca, A. Napolitano, S. Ito, *Pigm. Cell Res.* **2015**, *28*, 520–544.
- [3] Á. Molnár, *ChemCatChem* **2020**, *12*, 2649–2689.
- [4] a) H. Wang, J. Wu, C. Cai, J. Guo, H. Fan, C. Zhu, H. Dong, N. Zhao, J. Xu, *ACS Appl. Mater. Interfaces* **2014**, *6*, 5602–5608; b) M. Iacolino, J. I. Paez, R. Avolio, A. Carpentieri, L. Panzella, G. Falco, E. Pizzo, M. E. Errico, A. Napolitano, A. del Campo, M. d'Ischia, *Langmuir* **2017**, *33*, 2096–2102; c) Y. Long, L. Xiao, Q. Cao, *Powder Technol.* **2017**, *310*, 24–34; d) S. Suárez-García, J. Sedó, J. Saiz-Poseu, D. Ruiz-Molina, *Biomimetics* **2017**, *2*; e) S. Chen, J. Zhang, Y. Chen, S. Zhao, M. Chen, X. Li, M. F. Maitz, J. Wang, N. Huang, *ACS Appl. Mater. Interfaces* **2015**, *7*, 24510–24522; f) S. Chen, X. Li, Z. Yang, S. Zhou, R. Luo, M. F. Maitz, Y. Zhao, J. Wang, K. Xiong, N. Huang, *Colloids Surf. B* **2014**, *113*, 125–133.
- [5] J. Yang, V. Saggiomo, A. H. Velders, M. A. Cohen Stuart, M. Kamperman, *PLoS One* **2016**, *11*, e0166490.
- [6] a) F. Bernsmann, B. Frisch, C. Ringwald, V. Ball, *J. Colloid Interface Sci.* **2010**, *344*, 54–60; b) H. Lee, J. Rho, P. B. Messersmith, *Adv. Mater.* **2009**, *21*, 431–434.
- [7] a) Z. Lin, S. Luo, D. Xu, S. Liu, N. Wu, W. Yao, X. Zhang, L. Zheng, X. Lin, *Analyst* **2020**, *145*, 424–433; b) B. Silvestri, G. Vitiello, G. Luciani, V. Calcagno, A. Costantini, M. Gallo, S. Parisi, S. Paladino, M. Iacolino, G. D'Errico, M. F. Caso, A. Pezzella, M. d'Ischia, *ACS Appl. Mater. Interfaces* **2017**, *9*, 37615–37622; c) Z. Wang, M. Han, J. Zhang, F. He, Z. Xu, S. Ji, S. Peng, Y. Li, *Chem. Eng. J.* **2019**, *360*, 299–312; d) F. Chen, Y. Xing, Z. Wang, X. Zheng, J. Zhang, K. Cai, *Langmuir* **2016**, *32*, 12119–12128; e) N. T. Tran, D. P. Flanagan, J. A. Orlicki, J. L. Lenhart, K. L. Proctor, D. B. Knorr, *Langmuir* **2018**, *34*, 1274–1286; f) Y. Fu, M. Cai, E. Zhang, S. Cao, P. Ji, *Ind. Eng. Chem. Res.* **2016**, *55*, 4482–4489; g) F. Zhou, J. Luo, S. Song, Y. Wan, *Ind. Eng. Chem. Res.* **2020**, *59*, 2708–2717; h) D. B. Knorr, N. T. Tran, K. J. Gaskell, J. A. Orlicki, J. C. Woicik, C. Jaye, D. A. Fischer, J. L. Lenhart, *Langmuir* **2016**, *32*, 4370–4381.
- [8] M. Massaro, V. Campisciano, C. Viseras Iborra, L. F. Liotta, M. Sánchez-Polo, S. Rielma, M. Gruttadauria, *Nanomaterials* **2020**, *10*, 1416.
- [9] A. E. Fernandes, A. M. Jonas, *Catal. Today* **2019**, *334*, 173–186.
- [10] a) M. M. Heravi, F. Janati, V. Zadsirjan, *Monatsh. Chem.* **2020**, *151*, 439–482; b) F. Liang, Y.-J. Pu, T. Kurata, J. Kido, H. Nishide, *Polymer* **2005**, *46*, 3767–3775; c) L. F. Tietze, N. Rackelmann, *Pure Appl. Chem.* **2004**, *76*, 1967–1983; d) M. Zahouily, M. Salah, B. Bahlaouane, A. Rayadh, A. Houmam, E. A. Hamed, S. d Sebti, *Tetrahedron* **2004**, *60*, 1631–1635; e) T. Felbeck, S. Moss, A. M. P. Botas, M. M. Lezhnina, R. A. S. Ferreira, L. D. Carlos, U. H. Kynast, *Colloids Surf. B* **2017**, *157*, 373–380; f) Y.-T. Chen, C.-Y. Lin, G.-H. Lee, M.-L. Ho, *CrystEngComm* **2015**, *17*, 2129–2140; g) R. Banerjee, S. Mondal, P. Purkayastha, *RSC Adv.* **2016**, *6*, 105347–105349; h) R. Zhou, Z. Jiang, C. Yang, J. Yu, J. Feng, M. A. Adil, D. Deng, W. Zou, J. Zhang, K. Lu, W. Ma, F. Gao, Z. Wei, *Nat. Commun.* **2019**, *10*, 5393; i) K. van Beurden, S. de Koning, D. Molendijk, J. van Schijndel, *Green Chem. Lett. Rev.* **2020**, *13*, 349–364.
- [11] S. H. Hong, S. Hong, M.-H. Ryou, J. W. Choi, S. M. Kang, H. Lee, *Adv. Mater. Interfaces* **2016**, *3*, 1500857.
- [12] A. Corma, S. Iborra, I. Rodriguez, F. Sánchez, *J. Catal.* **2002**, *211*, 208–215.
- [13] M. Oubaha, M. Dubois, B. Murphy, P. Etienne, *J. Sol-Gel Sci. Technol.* **2006**, *38*, 111–119.
- [14] R. Tacke, A. Lopez Mras, J. Sperlich, C. Strohmman, W. F. Kuhs, G. Mattern, A. Sebald, *Chem. Ber.* **1993**, *126*, 851–861.
- [15] J. Liu, W. Mu, J. Wang, H. Liu, Y. Qin, J. He, F. Guo, Y. Li, Y. Li, X. Cao, P. Zhang, E. Lu, *Sep. Purif. Technol.* **2018**, *205*, 140–150.

- [16] B. Kannan, D. A. Higgins, M. M. Collinson, *Langmuir* **2012**, *28*, 16091–16098.
- [17] P. Pengthamkeerati, T. Satapanajaru, O. Singchan, *J. Hazard. Mater.* **2008**, *153*, 1149–1156.
- [18] a) J. Yang, M. A. Cohen Stuart, M. Kamperman, *Chem. Soc. Rev.* **2014**, *43*, 8271–8298; b) S. Haemers, G. J. M. Koper, G. Frens, *Biomacromolecules* **2003**, *4*, 632–640; c) S. W. Weidman, E. T. Kaiser, *J. Am. Chem. Soc.* **1966**, *88*, 5820–5827.
- [19] S. Patai, J. Zabicky, *J. Chem. Soc.* **1960**, 2030–2038.
- [20] E. V. Dalessandro, H. P. Collin, L. G. L. Guimarães, M. S. Valle, J. R. Pliego, *J. Phys. Chem. B* **2017**, *121*, 5300–5307.
- [21] a) R. Wirz, D. Ferri, A. Baiker, *Langmuir* **2006**, *22*, 3698–3706; b) G. Jones, *Org. React.* **1967**, *15*, 204–599.
- [22] a) E. Angeletti, C. Canepa, G. Martinetti, P. Venturello, *J. Chem. Soc. Perkin Trans. 1* **1989**, 105–107; b) D. Blasco-Jiménez, I. Sobczak, M. Ziolek, A. J. López-Peinado, R. M. Martín-Aranda, *Catal. Today* **2010**, *152*, 119–125; c) B. List, *Angew. Chem. Int. Ed.* **2010**, *49*, 1730–1734; *Angew. Chem.* **2010**, *122*, 1774–1779; d) X. Zhang, E. S. Man Lai, R. Martín-Aranda, K. L. Yeung, *Appl. Catal. A* **2004**, *261*, 109–118; e) D. Brunel, A. C. Blanc, A. Galarneau, F. Fajula, *Catal. Today* **2002**, *73*, 139–152.
- [23] S. M. Ribeiro, A. C. Serra, A. M. d. A. R. Gonsalves, *Appl. Catal. A* **2011**, *399*, 126–133.
- [24] a) I. Rodríguez, G. Sastre, A. Corma, S. Iborra, *J. Catal.* **1999**, *183*, 14–23; b) G. Jones, *Org. React.* **1967**, *15*, 204–599.
- [25] N. Al-Haq, R. Ramnauth, S. Kleinebiekel, D. Li Ou, A. C. Sullivan, J. Wilson, *Green Chem.* **2002**, *4*, 239–244.
- [26] a) M. Gruttadauria, F. Giacalone, A. Mossuto Marculescu, P. Lo Meo, S. RIELA, R. Noto, *Eur. J. Org. Chem.* **2007**, *2007*, 4688–4698; b) M. Gruttadauria, A. M. P. Salvo, F. Giacalone, P. Agrigento, R. Noto, *Eur. J. Org. Chem.* **2009**, *2009*, 5437–5444; c) M. Gruttadauria, F. Giacalone, A. M. Marculescu, R. Noto, *Adv. Synth. Catal.* **2008**, *350*, 1397–1405.
- [27] S. L. Hruby, B. H. Shanks, *J. Catal.* **2009**, *263*, 181–188.
- [28] a) D. A. Shirley, *Phys. Rev. B* **1972**, *5*, 4709–4714; b) P. M. A. Sherwood, in *Practical Surface Analysis* (Ed.: M. P. S. D. Briggs), Wiley, New York, **1990**, 190.
- [29] A. Nezamzadeh-Ejhieh, H. Zabihi-Mobarakeh, *J. Ind. Eng. Chem.* **2014**, *20*, 1421–1431.

Manuscript received: July 14, 2021

Revised manuscript received: September 20, 2021

Accepted manuscript online: September 21, 2021

Version of record online: October 13, 2021